Near IR Nonlinear Absorbing Chromophores with Optical Limiting Properties at Telecommunication Wavelengths

Pierre-Antoine Bouit,[†] Guillaume Wetzel,[‡] Gérard Berginc,[⊥] Brigitte Loiseaux,[‡] Loïc Toupet,[#] Patrick Feneyrou,[‡] Yann Bretonnière,[†] Kenji Kamada,[§] Olivier Maury,*,[†] and Chantal Andraud*,[†]

Laboratoire de Chimie, UMR 5182 CNRS−Ecole Normale Supérieure de Lyon, 46 Allée d'Italie, F-69364 Lyon Cedex 07, France, Thales Research & Technology France, Route Départementale 128, 91767 Palaiseau Cedex, France, Thales Optronique SA, BP 55, Rue Guynemer, 78283 Guyancourt, France, Groupe de la Matière Condensée et Matériaux, UMR 6626 CNRS−Université de Rennes 1, Campus de Beaulieu, 35042 Rennes cedex, France, Photonics Research Institute, National Institute of Advanced Industrial Science and Technology, AIST Kansai Center, 1-8-31 Midorigaoka, Ikeda, Osaka 563-8577, Japan

Dipolar and symmetrical heptamethine dyes featuring strong linear absorption in the near-infrared spectral range (700−900 nm) were prepared at a gram scale. X-ray crystallographic structure of the dipolar chromophore is described revealing the remarkable planarity of the polyenic chain due to the central ring of the molecule. These chromophores present promising nonlinear absorption properties at telecommunication wavelengths (1400−1600 nm): (i) significant two-photon cross-sections were measured using the femtosecond Z-scan method, and (ii) their exceptional solubility allows us to carry out an optical-limiting experiment at 1500 nm in the nanosecond regime. In this regime, experimental data were interpreted on the basis of two-photon absorption (2PA) and 2PA-induced excited-state absorption (ESA). Finally, these systems, which present a lot of relevant properties (significant nonlinear absorption properties, two-step gram scale synthesis, high solubility, good thermal stability, and several sites of functionalization), open the way to numerous practical applications in biology, solid-state optical limiting, and signal processing.

Introduction

Materials displaying multiphotonic absorption properties have been extensively studied for applications in the field of material science (optical storage, optical limitation, microfabrication) or in biology (imaging, drug delivery, photodynamic therapy) generally using a femtosecond-pulsed laser source emitting in the visible range (400−900 nm).[1] The rapid development of frequency-tuneable pulsed laser up to telecommunication wavelengths (1400−1600 nm) prompted the scientific community to the design of new materials for nonlinear absorption in the near infrared region (NIR). In this spectral range, such materials could address various applications for optical limiting (OL), such as gain equalization of Erbium amplifier for telecommunication systems, protection of monostatic LIDAR (light detection and ranging) detectors against intense retro-reflection/back-scattering (in addition to or replacement of detector gating), and protection of active imagery systems against laser threat. A good OL device should be able to protect optical sensors like eyes or camera against damages caused by high-energy laser illumination; it has to be transparent in the spectral

range of the detector as long as the light intensity remains below the sensor safety threshold and to instantaneously attenuate the beam when its intensity exceeds this threshold.[2] Most of the OL studies reported to date deal with laser emitting in the visible range (400−1000 nm), where the nonlinear transmission phenomena are mainly based on

* Corresponding author. E-mail: chantal.andraud@ens-lyon.fr (C.A.); patrick.feneyrou@thalesgroup.com (P.F.); k.kamada@aist.go.jp (K.K.).
[†] Ecole Normale Supérieure de Lyon.
[‡] Thales Research & Technology France.
[⊥] Thales Optronique SA.
[#] Université de Rennes 1.
[§] National Institute of Advanced Industrial Science and Technology.

(1) For selected examples of two-photon applications, see: (a) Cumpston, B. H.; Ananthavel, S. P.; Barlow, S.; Dyer, D. L.; Ehrlich, J. E.; Erskine, L. L.; Heikal, A. A.; Kuebler, S. M.; Sandy-Lee, I.-Y.; McCord-Maughon, D.; Qin, J.; Röckel, H.; Rumi, M.; Wu, X.-L.; Marder, S. R.; Perry, J. R. *Nature* **1999**, *398*, 51−54. (b) Wang, S.; Gang, Q.; Zhang, Y.; Li, S.; Xu, H.; Yang, G. *Chem. Phys. Chem.* **2006**, *7*, 935−941. (c) Dini, D.; Calvete, M. J. F.; Hanack, M.; Amendola, V.; Meneghetti, M. *Chem. Commun.* **2006**, 2394−2396. (d) Anémian, R.; Morel, Y.; Baldeck, P. L.; Paci, B.; Kretsch, K.; Nunzi, J.-M.; Andraud, C. *J. Mater. Chem.* **2003**, *13*, 2157−2163. (e) Kawata, S.; Sun, H.-B.; Tanaka, T.; Takada, K. *Nature* **2001**, *412*, 697−698. (f) Belfield, K. D.; Ren, X.; Van Stryland, E. W.; Hagan, D. J.; Dubikovsky, V.; Miesak, E. J. *J. Am. Chem. Soc.* **2000**, *122*, 1217−1218. (g) Klein, S.; Barsella, A.; Leblond, H.; Bulou, H.; Fort, A.; Andraud, C.; Lemercier, G.; Mulatier, J. C.; Dorkenoo, K. *Appl. Phys. Lett.* **2005**, *86*, 211118. (h) Yuste, R. *Nat. Methods* **2005**, *2*, 902−904. (i) Campagnola, P. J.; Loew, L. M. *Nature Biotechnol.* **2003**, *21*, 1356−1360. (j) Zipfel, W. R.; Williams, R. M.; Webb, W. W. *Nature Biotechnol.* **2003**, *21*, 1356−1360. (k) Nikolenko, V.; Yuste, R.; Zayat, L.; Baraldo, L. M.; Etchenique, R. *Chem. Commun.* **2005**, 1752−1754. (l) Wecksler, S. R.; Mikhailowsky, A.; Korystov, D.; Ford, P. C. *J. Am. Chem. Soc.* **2006**, *128*, 3831−3837. (m) Fredericksen, P. K.; Jorgensen, M.; Ogilby, P. R. *J. Am. Chem. Soc.* **2001**, *123*, 1215−1221. (n) Oar, M. A.; Serin, J. M.; Dichtel, W. R.; Fréchet, J. M. J.; Ohulchanskyy, T. Y.; Prasad, P. N. *Chem. Mater.* **2005**, *17*, 2267−2275.

(2) For a review, see: Spangler, C. W. *J. Mater. Chem.* **1999**, *9*, 2013−2020 and references therein.

5326 *Chem. Mater., Vol. 19, No. 22, 2007*

Bouit et al.

multiphotonic absorption, reverse saturable absorption, or nonlinear scattering and the materials designed for such purpose are generally organic molecules, e.g., fullerene, carbon nanotube, (oligo)-fluorene-based chromophores, met-allo-porphyrines or phtalocyanines, and organometallic complexes.[2d,3] It is important to note that the NIR spectral region has been less investigated. To date, inorganic semi-conductors are known to present a significant two-photon absorption (2PA) coefficient (α_2) of 1.9×10^{-10} m W^{-1} at 1300 nm;[4] as far as organic systems are concerned, only a few works have been reported: Marder and co-workers reported bis-dioxaborine polymethine-based materials with large microscopic and macroscopic third-order nonlinearities at 1300 nm, dipolar chromophores with a 2PA response in the NIR wavelengths range,[5] and extended conjugated quadrupolar chromophores with strong 2PA properties centered around 1000 nm,[6] but with additional properties at telecommunications wavelengths.[7] In the same context, fused azulene and oligomeric porphyrins were also shown to exhibit large 2PA cross-sections between 1200 and 1400 nm,[8] whereas singlet diradical compounds[9] and nickel bis(diothi-olene) complexes exhibit properties at telecommunications wavelengths.[10] On the other hand, the group of Prasad recently described OL measurements at 1300 nm on the basis of three-photon absorption properties using linear or multi-branched chromophores, with a maximal nonlinear transmit-tance of nearly 0.7.[11] Finally, OL by reverse saturable absorption was observed at 1315 nm in fullerene-doped polyimides.[12]

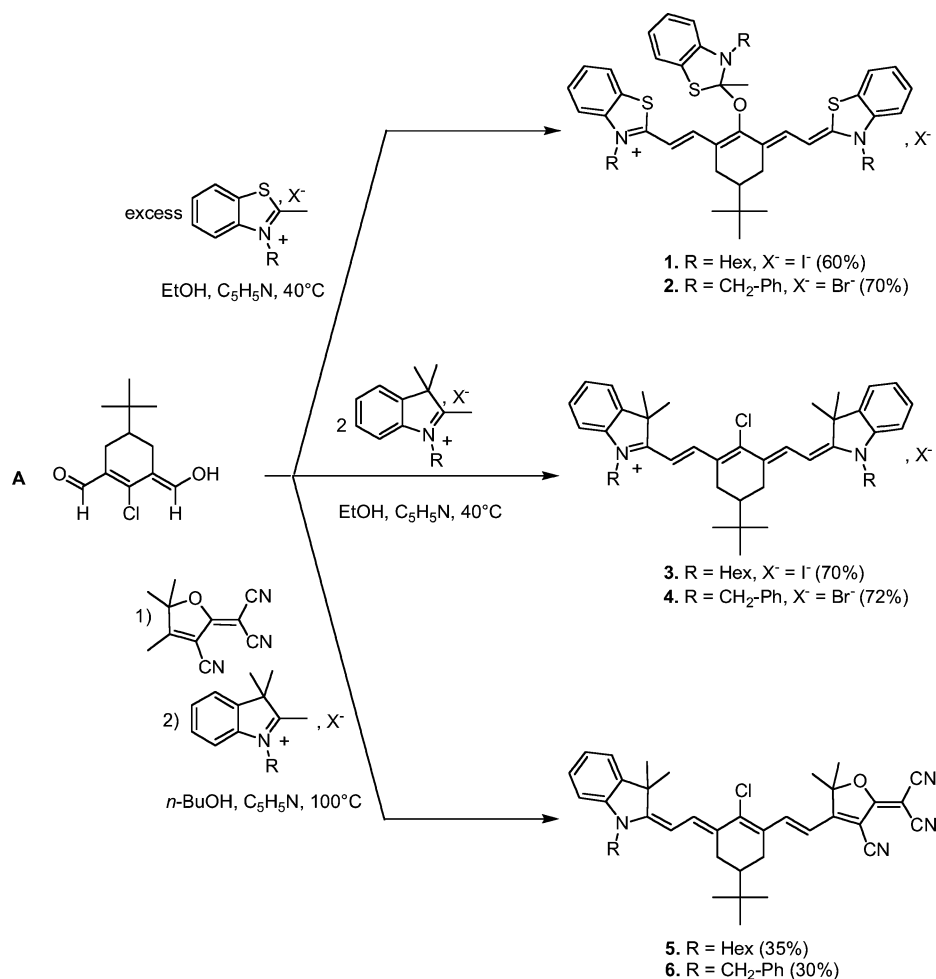The observation of an efficient 2PA process at the wavelength λ requires the design of chromophores with a linear absorption at least at higher wavelength than $\lambda/2$. In the present case for 2PA in the 1400−1600 nm range, target chromophores have to present an intense linear absorption at wavelengths larger than 700−800 nm. Furthermore, to be used for practical applications, an additional set of specific conditions must be fulfilled: (i) a large solubility in organic solvents, (ii) a good thermal and photophysical stability, and (iii) a synthesis achieved at a gram scale, which is a real challenge for highly conjugated molecules. For that purpose, we focused on symmetrical heptamethine chromophores,[13] largely used in biological imaging applications for their particular absorption in the near-IR region (700−900 nm)[14] and on new dipolar related compounds. Target dyes **1−6** (Scheme 1) present a polyenic backbone locked in a cyclohexyl ring to increase the photostability; in addition, all the compounds are functionalized by hexyl or benzyl fragments to increase their solubility and by a lateral bulky *tert*-butyl group to prevent aggregation. Keeping in mind further practical applications, the preparation of dyes **1−6** requires only a few steps and the synthesis can be achieved on a gram scale. In this article, we report on the synthesis and chemical characterization of these six dyes; the X-rays structure of a new dipolar chromophore is also depicted. 2PA properties of these dyes in the NIR spectral range (1300−1600 nm) were determined using the Z-scan technique in the femtosecond regime, and optical limiting studies were performed in the nanosecond regime. It is also worth noting that this paper described the first optical-limiting properties of organic dyes at the telecommunications wavelength of 1500 nm, which is of prime importance for further practical applications.

Results and Discussion

Synthesis and Characterization. The *tert*-butyl function-alized chloro-bis-aldehyde **A**[15] is the common starting material for the synthesis of chromophores **1−6**. The heptamethine dyes **1−4** were classically prepared on a gram scale by condensation of **A** with benzothiazolium or indo-lenium salts under mild experimental conditions.[16] Whereas condensation of **A** with 2 equiv. of indolenium salt gave the expected 2/1 adduct as the only product, reaction with benzothiazolium salts mainly led to the formation of a 3/1 adduct. This new product results from the substitution of the lateral chloride atom by 2-hydroxyl-benzothiazole formed

(3) For selected examples see: (a) Cha, M.; Saricifti, N. S.; Heeger, A. J.; Hummelen, J. C.; Wudl, F. *App. Phys. Lett.* **1995**, *67*, 3850−3853. (b) Morel, Y.; Irimia, A.; Najechalski, P.; Kervella, Y.; Stephan, O.; Baldeck, P. L.; Andraud, C. *J. Chem. Phys.* **2001**, *114*, 5391−5396. (c) Anémian, R; Mulatier, J. C.; Andraud, C.; Morel, Y.; Stephan, O.; Baldeck, P. L. *Proc. SPIE* **2002**, *4797*, 25−33. (d) Charlot, M.; Izard, N.; Mongin, O.; Riehl, D.; Blanchard-Desce, M. *Chem. Phys. Lett.* **2006**, *417*, 297−302. (e) Dini, D.; Calvete, M. J. F.; Hanack, M.; Amendola, V.; Meneghetti, M. *Chem. Commun.* **2006**, 2394−2396. (f) Wang, S.; Gan, Q., Zhang, Y.; Li, S.; Xu, H.; Yang, G. *Chem. Phys. Chem.* **2006**, *7*, 935−941. (g) McEwan, K.; Lewis, K.; Yang, G.-Y.; Chng, L. L.; Lee, Y.-W; Lau, W.-P.; Lai, K.-S. *Adv. Funct. Mater.* **2003**, *13*, 863−867. (h) Zhou, G.-J.; Wong, W.-Y.; Lin, Z.; Ye, C. *Angew. Chem., Int. Ed.* **2006**, *45*, 6189−6193.
(4) Van Stryland, E.; Woodall, M. A.; Van der Zeele, H.; Soileau, M. J. *Opt. Lett.* **1985**, *10*, 490−492.
(5) (a) Hales, J. H.; Zheng, S.; Barlow, S.; Marder, S. R.; Perry, J. W. *J. Am. Chem. Soc.* **2006**, *128*, 11362−11363. (b) Beverina, L.; Fu, J.; Leclercq, A.; Zojer, E.; Pacher, P.; Barlow, S.; Van Stryland, E. W.; Hagan, D. J.; Brédas, J.-L.; Marder, S. R. *J. Am. Chem. Soc.* **2005**, *127*, 7282−7283.
(6) Zheng, S.; Leclercq, A.; Fu, J.; Beverina, L.; Padilha, L. A.; Zojer, E.; Schmidt, K.; Barlow, S.; Luo, J.; Jiang, S.-H.; Jen, A. K.-Y.; Yi, Y.; Shuai, Z.; Van Stryland, E. W.; Hagan, D. J.; Bredas, J. L.; Marder, S. R. *Chem. Mater.* **2007**, *19* (3), 432−442.
(7) Chung, S.-J.; Zheng, S.; Odani, Y.; Beverina, L.; Fu, J.; Padilha, L. A.; Biesso, A.; Hales, J. M.; Zhan, X.; Schmidt, K.; Ye, A.; Zojer, E.; Barlow, S.; Hagan, D. J.; Van Stryland, E. W.; Yi, Y.; Shuai, Z.; Pagani, G. A.; Brédas, J.-L.; Perry, J. W.; Marder, S. R. *J. Am. Chem. Soc.* **2006**, *128*, 14445−14446.
(8) (a) Kurotobi, K.; Kim, K. S.; Noh, S. B.; Kim, D.; Osuka, A. *Angew. Chem., Int. Ed.* **2006**, *45*, 3944−3947. (b) Drobizhev, M.; Stepanenko, Y.; Rebane, A.; Wilson, C. J.; Screen, T. E. O.; Anderson, H. L. *J. Am. Chem. Soc.* **2006**, *128*, 12432−12433.
(9) Kamada, K.; Ohta, K.; Kubo, T.; Shimizu, A.; Morita, Y.; Nakasuji, K.; Kishi, R.; Ohta, S.; Furukawa, S.-I.; Takahashi, H.; Nakano, M. *Angew. Chem., Int. Ed.* **2007**, *46*, 3544−3546.
(10) Cho, J. Y.; Barlow, S.; Marder, S. R.; Fu, J.; Padiha, L. A.; Van Stryland, E. W.; Bishop, M. *Opt. Lett.* **2007**, *32*, 671−673.
(11) (a) Lin, T.-C.; He, G. S.; Zheng, Q.; Prasad, P. R. *J. Mater. Chem.* **2006**, *16*, 2490−2498. (b) Zheng, Q.; He, G. S.; Lu, C.; Prasad, P. N. *J. Mater. Chem.* **2005**, *16*, 3488−3493.
(12) (a) Kamanina, N. V.; Bagrov, I. V.; Belousova, I. M.; Kognovitskii, S. O.; Zhevlakov, A. P. *Opt. Commun.* **2001**, *194*, 367−372. (b) Kamanina, N. V.; Voronin, Y. M.; Varnaev, A. V.; Bagrov, I. V.; Zhevlakov, A. P. *Synth. Met.* **2003**, *138*, 317−322.
(13) For a general review on cyanine dyes see: Mishra, A.; Behera, R. K.; Behera, P. K.; Mishra, B. K.; Behera, G. B. *Chem. Rev.* **2000**, *100*, 1973−2011.
(14) (a) Kiyose, K.; Kojima, H.; Urano, Y.; Nagano, T. *J. Am. Chem. Soc.* **2006**, *128*, 6548−654. (b) Li, C.; Greenwood, T. R.; Bhujwalla, Z. M.; Glunde, K. *Org. Lett.* **2006**, *8*, 3623−3626. (c) Peng, X.; Song, F.; Lu, E.; Wang, Y.; Zhou, W.; Fan, J.; Gao, Y. *J. Am. Chem. Soc.* **2005**, *127*, 4170−4171. (d) Sasaki, E.; Kojima, H.; Nishimatsu, H.; Urano, Y.; Kikuchi, K.; Hirata, Y.; Nagano, T. *J. Am. Chem. Soc.* **2005**, *127*, 3684−3685 and references therein.
(15) Reynolds, G. A.; Drexhage, K. H. *J. Org. Chem.* **1977**, *42*, 885−888.
(16) Narayan, N.; Patonay, G. *J. Org. Chem.* **1995**, *60*, 2391−2395.

Scheme 1. Synthesis of the Target Chromophores

1. R = Hex, X⁻ = I⁻ (60%)
2. R = CH₂-Ph, X⁻ = Br⁻ (70%)

3. R = Hex, X⁻ = I⁻ (70%)
4. R = CH₂-Ph, X⁻ = Br⁻ (72%)

5. R = Hex (35%)
6. R = CH₂-Ph (30%)

in situ by addition of a water molecule liberated during the first condensation to the starting salt.[17] This 3/1 adduct is the only product formed in the presence of an excess of benzothiazolium salt and was isolated in good yield. On the other hand, the dipolar chromophores **5−6** were obtained in a one-pot, two-step procedure by successive additions of tricyanofurane and indolenium salt to **A** using more drastic experimental conditions (Scheme 1).[18] It is worth noting that both dipolar chromophores are chiral; the carbon carrying the ᵗBu fragment, noted C4 on the ORTEP drawing (vide infra), is asymmetric, but only racemic mixtures were considered. All these compounds (**1−6**) are very soluble in all common organic solvents and were isolated as green microcrystalline powder in good to moderate yields after recrystallization or column chromatography. Complete characterization is provided in the experimental section; ¹H NMR spectra of **3−4** (Figure 1) exhibit only two signals (doublet) for the vinylic proton indicating a C_{2v} symmetric architecture of the molecule with a complete delocalization of the cationic charge over the π-conjugated backbone. These signals are slightly modified for compounds **1−2**; each doublet is divided in two, the hindered free rotation of the lateral bulky

benzothiazole substituent breaking the C_{2v} symmetry. Finally, the polyenic chain of the dipolar compounds **5−6** presents two different sets of signals in agreement with an asymmetric structure. It is worth noting that, in all cases, the vinylic $^{3}J_{H-H}$ coupling constant, between 13 and 16 Hz, unambiguously indicates the all-trans configuration of the sp² carbon squeleton. All compounds are thermally robust with 10% weight loss decomposition temperature between 210 and 280 °C (Table 1), which is of prime importance for further applications. It is worth noting that benzothiazole derivatives **1−2**, exhibiting the lowest decomposition temperature, also present the lowest chemical stability.[19]

X-rays Crystal Structure. Single crystals of **6** were obtained as thin needles, featuring metallic shine by slow evaporation of a toluene/chloroform mixture. Crystal data and refinement parameters are summarized in the Experimental Section. The dipolar chromophore crystallizes in a centrosymmetric space group and the crystal packing is composed of a stacking of linear chains of dimers (Figure 2a). The elementary dimeric unit is composed by the two different enantiomers, which can be distinguished by the blue and red colors in panels a and b of Figure 2a and are organized in a head-to-tail way. The intermolecular interac-

(17) Ramos, S. S.; Santos, P. F.; Reis, L. V.; Almeida, P. *Dyes Pigm.* **2002**, *53*, 143−152.

(18) Related dipolar compounds have been already reported but they feature very low solubility: Kay, A. J.; Woolhouse, A. D.; Zhao, Y.; Clays, K. *J. Mater. Chem.* **2004**, *14*, 1321−1330.

(19) For instance, both compounds featuring benzothiazole fragments rapidly decomposed on column chromatography over silica or alumina, certainly due to the presence of the reactive sulphur atoms.

5328 *Chem. Mater., Vol. 19, No. 22, 2007*

Bouit et al.
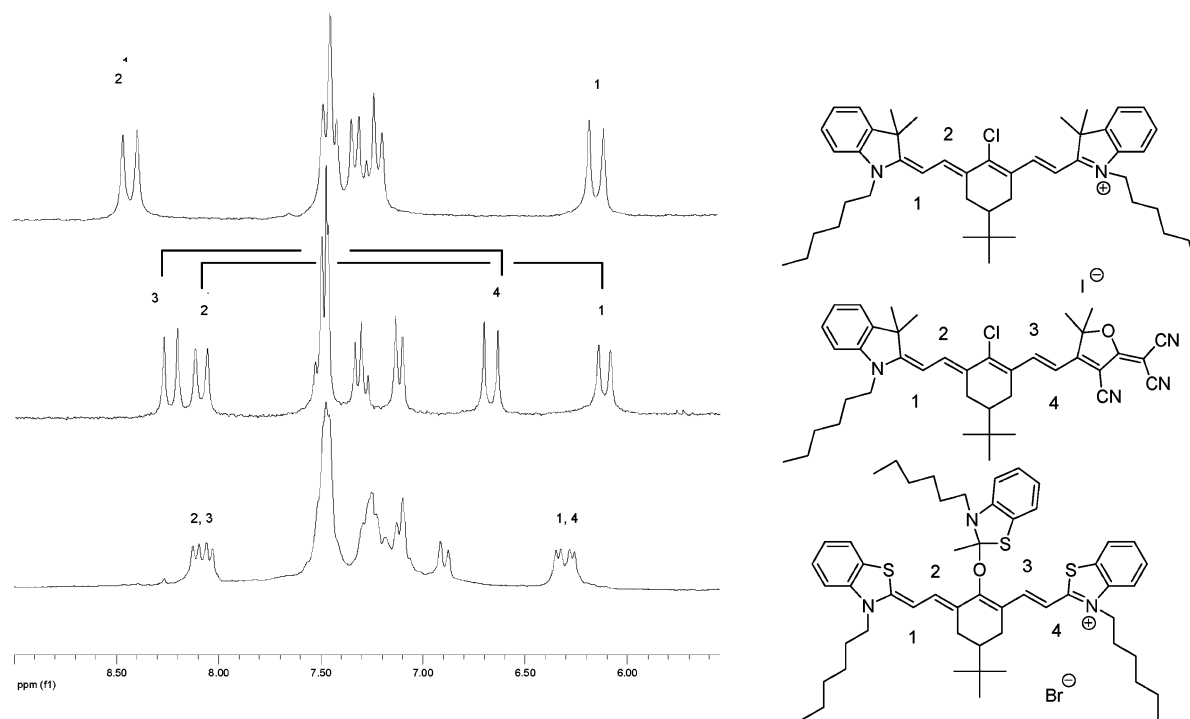
Figure 1. Comparison of the aromatic region of the ^{1}H NMR spectra (200.13 MHz, CDCl3, RT) for **3** (top), **5** (middle), and **1** (bottom).

Table 1. Photophysical Data in Dichloromethane Solution

compd	λ_{max} (nm)	ϵ_{max} (L mol^{-1} cm^{-1})	$\lambda^{(2)}$ (nm)^a	σ_{2PA}^{max} (GM)^b	T_{d5-10} (°C)^c
1	825	240 000			200−210
2	833	270 000	1495	544	205−225
3	791	355 000			240−245
4	794	350 000	1437	731	240−245
5	831	112 000			225−250
6	810	91 000	1445	792	274−277

^{a} Maximal two-photon absorption wavelength. ^{b} Maximal two-photon absorption cross-section measured by femtosecond Z-scan technique. ^{c} Decomposition temperature at 5 and 10% weight loss, quoted to the 5 °C inferior, measured by thermogravimetric analysis (TGA) under nitrogen.

tion seems to be driven by the steric repulsion ensured by the benzyl and *tert*-butyl fragment resulting in a closed packing between two cyano functions of the tricyanofurane acceptor group ($d \approx 3.1-3.2$ Å). The intrachain cohesion is ensured by hydrogen bonds between the cyano acceptor fragment and a benzenic proton of a donor group inducing a D−A···D−A intrachain organization. Finally, the inter-chain interactions (with the green molecule in panels a and b in Figure 2) originate from C−H···Cl interactions ($d = 2.9$ Å) between the methyl fragment of the dimethylindole moieties and the chlorine atom resulting in a quasi-orthogonal arrangement of two neighboring chains (Figure 2b). On the molecular scale, the ORTEP drawing (Figure 2c for one enantiomer) reveals a perfectly planar structure without any significant twist of the polyenic chain, the overall tilt angle between the phenyl donor and the tricyanofurane acceptor plane being only about 10°. This remarkable planarity is mainly due to the presence of the central six-membered ring containing three sp^2 carbon atoms, whose conformation is further constrained by the most stable equatorial position of the *tert*-butyl fragment. The all-trans 12 sp^2 carbons back-bone, linking the amino donor to the cyano acceptor groups, presents a very regular alternance of single and double bonds,

whose average lengths are 1.425 and 1.364 Å, respectively.[20] These classical values confirm the strong dipolar character of the molecule with a complete delocalization over the extended π-conjugated skeleton.

Linear and Nonlinear Optical Properties. Absorption spectra of **1**−**4** in dichloromethane solution (Figure 3 and Table 1) are characteristic of cyanine-like derivatives,[10,21] i.e., a sharp electronic transition in the NIR region with a huge extinction coefficient (λ_{max} (**3**) = 791 nm, ϵ = 355 000 L mol^{-1} cm^{-1}) and a less intense shoulder at higher energy. As already described, chromophores featuring the stronger benzothiazole donating group (**1**, **2**), present the most red-shifted absorption wavelength (λ_{max} (**1**) = 825 nm and λ_{max} (**2**) = 833 nm),[13] whereas dipolar compounds **5**−**6** exhibit a broad absorption band in the 600−900 nm range resulting from the overlap of two transitions.[22] It is important to note that the shape of these spectra remains unchanged when the concentration varies from 1×10^{-7} to 1×10^{-4} mol L^{-1}, and follows the Beer−Lambert law. This observation ex-cludes the possibility of aggregation effects within this concentration range and can be connected to the presence of the bulky ^{t}Bu fragment in the central part of the molecule and the benzyl- or alkyl-amine functionality.[10b,23]

Two-photon absorption spectra were measured by using an open aperture Z-scan method between 1200 and 1600 nm

(20) For other polyene crystal structures, see for example: (a) Shu, C.-F.; Shu, Y.-C.; Gong, Z.-H.; Peng, S.-M.; Lee, G.-H.; Jen, A. K. Y. *Chem. Mater.* **1998**, *10*, 3284−3286. (b) Brotin, T.; Andraud, C.; Ledoux, I.; Brasselet, S.; Zyss, J.; Perrin, M.; Thozet, A.; Collet, A. *J. Am. Chem. Soc.* **1996**, *118*, 890−906.
(21) Lepkowicz, R. S.; Przhonska, O. V.; Hales, J. M.; Fu, J.; Hagan, D. J.; Van Stryland, E. W.; Bondar, M. V.; Slominsky, Y. L.; Kachkovski, A. D. *Chem. Phys.* **2004**, *305*, 259−270.
(22) Detailed studies of the photophysical properties will be reported elsewhere.
(23) Asato, A. E.; Watanabe, D. T.; Liu, R. S. H. *Org. Lett.* **2000**, *2*, 2559−2562.
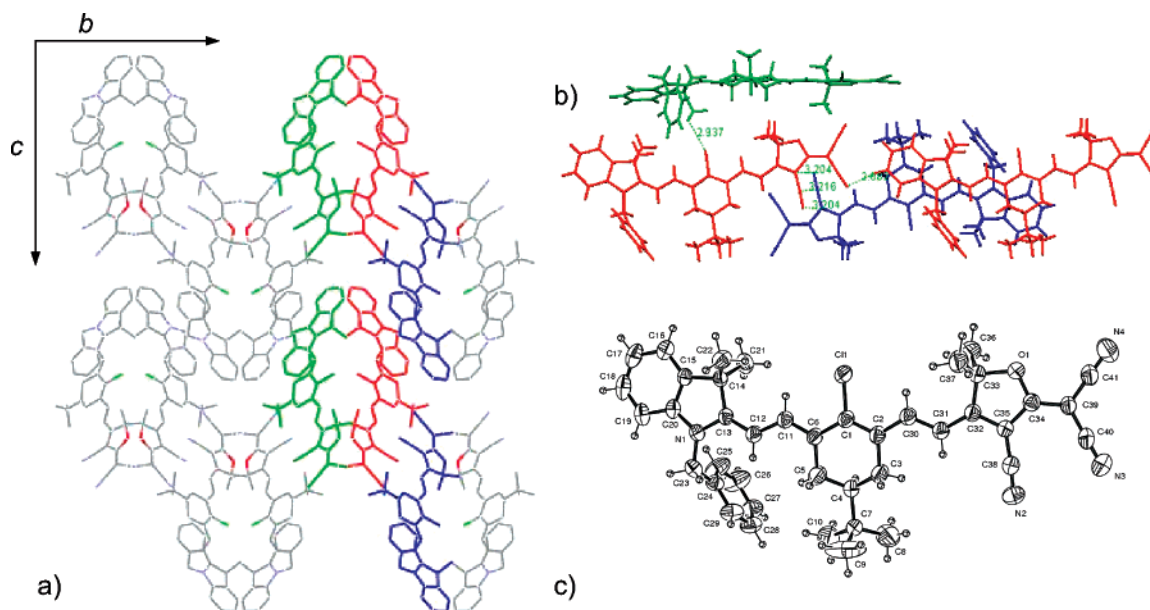
Figure 2. Crystallographic structure of **6**: (a) view of the crystal packink along the *a* axis; (b) details of the intermolecular interactions; (c) ORTEP drawing. Selected distances (Å) N(1)−C(13) 1.382 (3), C(13)−C(12) 1.360 (3), C(12)−C(11) 1.419 (3), C(11)−C(6) 1.358 (3), C(6)−C(1) 1.442 (3), C(1)−C(2) 1.360 (3), C(2)−C(30) 1.423 (3), C(30)−C(31) 1.363 (3), C(31)−C(32) 1.415 (3), C(32)−C(35) 1.369 (3), C(35)−C(34) 1.429 (3), C(34)−C(39) 1.378 (3).
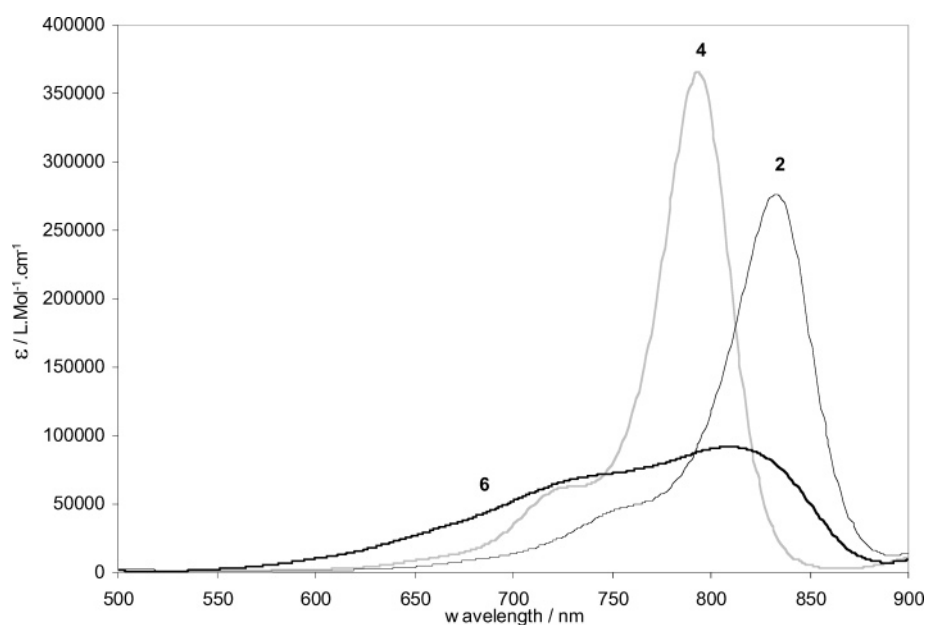
Figure 3. UV−vis−NIR absorption spectra for **2** (thin black), **4** (gray), and **6** (black) in dichloromethane.

with a fs-optical parametric amplifier pumped by a Ti: sapphire regenerative amplifier laser operating at 1 kHz as a light source. Typical pulse duration was 130 fs. Details of the setup were published previously.[24] At each wavelength, the open-aperture traces were recorded by changing the incident power of the laser beam from 0.1 to 0.7 mW corresponding to the on-axis peak intensity at the focal point I_0 of 7−80 GW cm^{-2} depending on the Rayleigh range (z_R = 11−14 mm). The sample solutions in spectroscopic grade dichloromethane (4−5 mol L^{-1}) poured in a 1-mm quartz cuvette were used for the measurements. The longer z_R than

the length of the sample (L = 1 mm) fulfills the optically thin condition.[25]

The basic theory for the analysis of the open-aperture Z-scan and the nonlinear transmittance measurements are the same. When a material absorbs light by only 1PA and 2PA processes and the cascading processes can be ignored, the transmission of the sample can be computed using the following eq. 1

$$\frac{dI}{dz} = -\alpha_1 I - \alpha_2 I^2 \qquad (1)$$

where I is the optical intensity, z is the propagation axis coordinate, and α_1 and α_2 are the 1PA (linear) and 2PA

(24) Kamada, K.; Matsunaga, K.; Yoshino, A.; Ohta, K. *J. Opt. Soc. Am. B* **2003**, *20*, 529−537.
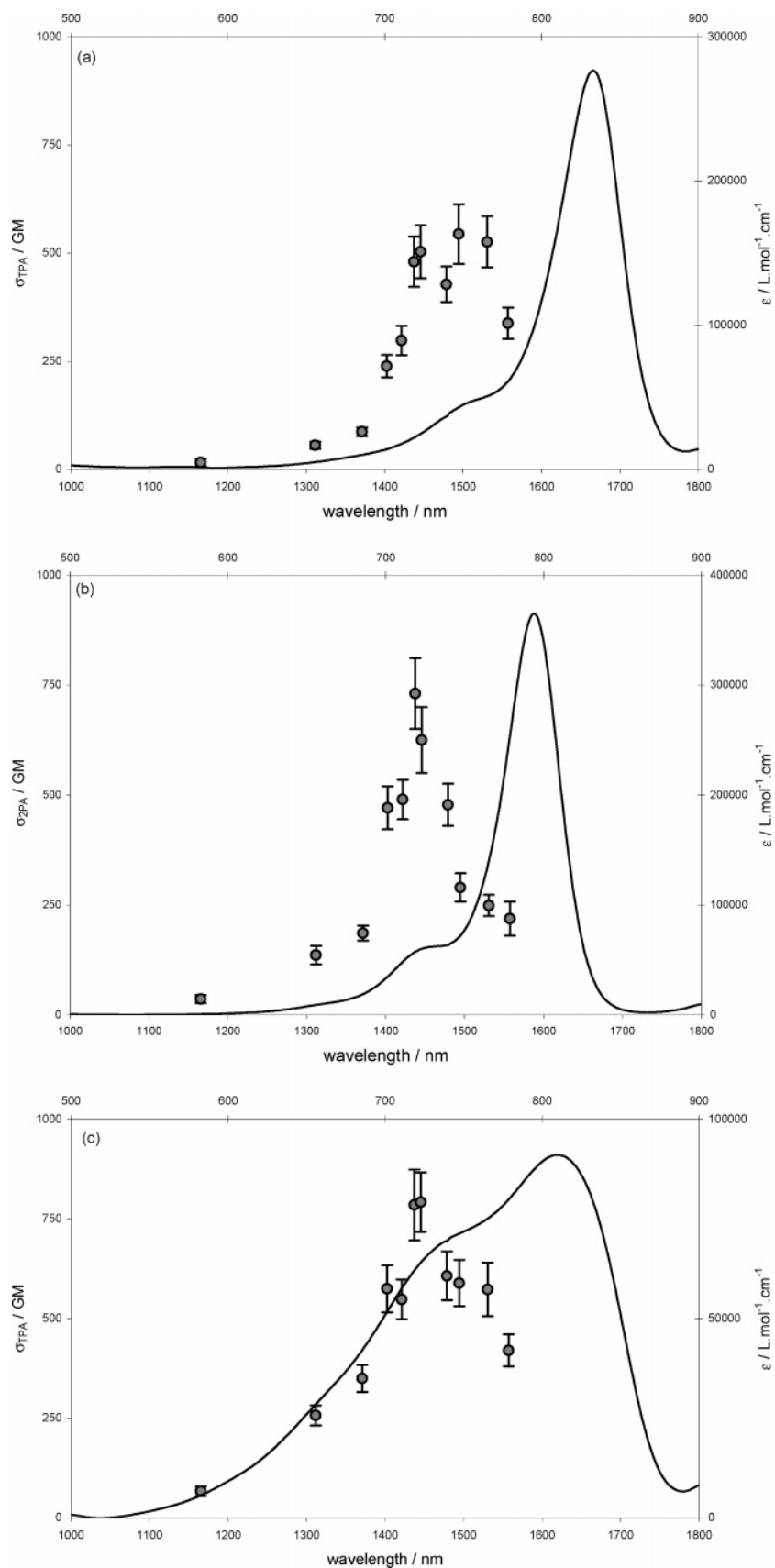
Figure 4. 2PA spectra measured by fs-Z-scan method (filled circle) and 1PA spectra in upper abscissa (—) of compounds (a) **2**, (b) **4**, and (c) **6** in dichloromethane solution.

absorption coefficients, respectively. Under the current experimental conditions, all solutions were transparent at the operating wavelengths ($\alpha_1 \approx 0$ cm^{-1}). Thus, the term including α_1 can be ignored and the eq. 1 become simplified as dI/d$z = -\alpha_2 I^2$. Considering the propagation of a collimated laser beam with a Gaussian distribution in time and
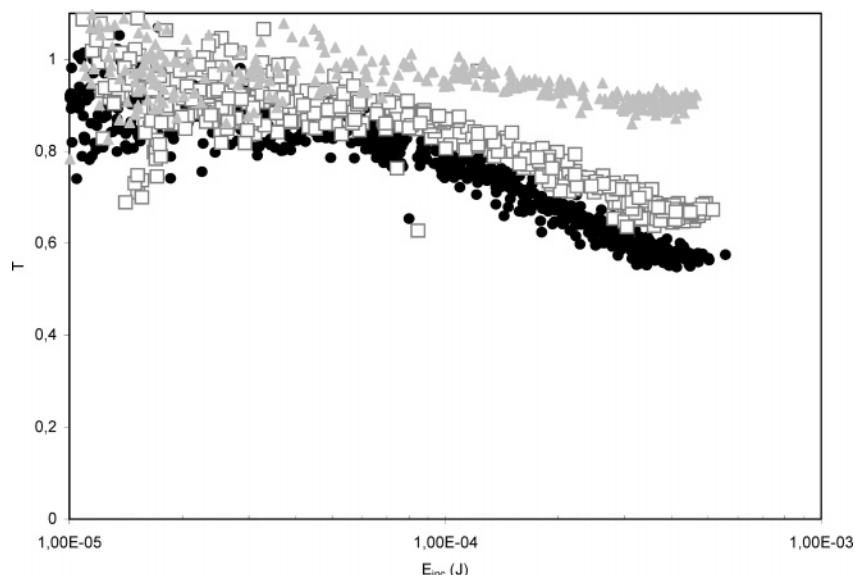
Figure 5. Nonlinear transmittance of **1** using 1500 nm as incident wavelength in dichloromethane solutions of different concentrations: $C_1 = 223.4$ g L^{-1} (gray triangle); $C_2 = 281.6$ g L^{-1} (open square); $C_3 = 320.4$ g L^{-1} (black circle).

space through a media having only 2PA, the nonlinear transmittance T_{nl} can be expressed by eq 2[26]

$$T_{nl} = \frac{1}{\sqrt{\pi}\alpha_2 LI} \int_{-\infty}^{\infty} \ln(1 + \alpha_2 LI e^{-u^2})\, du \qquad (2)$$

For the nonlinear transmittance measurements, this relation can be used as it is because I is the control parameter. Meanwhile, for the Z-scan experiments, T_{nl} is a function of a sample position z because I is now a function of z as $I(z) = I_0/(1 + (z/z_R)^2)$. By the curve fit with these relations to the recorded open-aperture traces, the value of α_2 was obtained. At some wavelength in the NIR region, the solvent has overtone of vibrational absorption. At such a wavelength, the depression of the incident power by the overtone was taken into account by replacing L in eq 2 with the effective path length $L_{eff} = (1 - e^{-\alpha_1 L})/\alpha_1$, where the 1PA coefficient of the solvent is used for α_1. The α_2 value obtained by this procedure did not change for the different values of I_0 employed, which guarantees that the α_2 obtained by the femtosecond Z-scan measurements contains negligible contribution by higher-order processes[27] such as the effective three-photon absorption, i.e., 2PA-induced excited-state absorption (ESA). Finally, the 2PA cross-section σ_{2PA} is calculated from the convention

$$\sigma_{2PA} = \frac{h\nu}{N}\alpha_2 \qquad (3)$$

where N is the number density of molecules and $h\nu$ is the photon energy at the operating wavelength.

Figure 4 shows the comparison of 2PA and 1PA spectra of compounds **2**, **4**, and **6** that all present significant 2PA absorption in the 1300−1500 nm range. The 2PA spectrum of the noncentrosymmetric dipolar compound (**6**) matches the wavelength-doubled scale 1PA absorption (Figure 4c). The case of the polymethine cyanines **2** and **4** (panels a and b in Figure 4) is different; the 2PA spectrum is blue-shifted with respect to the wavelength-doubled main transition of the 1PA spectrum and seems to match the weakest band. It is well-known that the selection rules for centrosymmetric molecules are complementary for 1PA and 2PA transitions: a 1PA-allowed transition is forbidden for 2PA transition and vice versa.[28] It is not clear to date why the 2PA peak overlaps with the weakest 1PA band, i.e., coincidence in the transition energies to 1PA- and 2PA-allowed excited states, or breaking of the centrosymmetry because of vibronic coupling or other reasons. Theoretical calculations are currently in progress for the assignment of these different transitions. All compounds present maximal 2PA wavelength $\lambda^{(2)}$ between 1430 and 1500 nm, and interestingly, **2**, which presents the most red-shifted 1PA wavelength, also exhibits the most red-shifted 2PA wavelength. The maximum two-photon cross-sections σ_{2PA}^{max} summarized in Table 1 are between 450 and 800 GM. The σ_{2PA}^{max} values obtained in the case of polymethine dyes **2** and, **4** compare well with that of related compounds briefly described in the literature.[29] The σ_{2PA}^{max} of the dipolar chromophore **6** is slightly higher ($\sigma_{2PA}^{max} = 792 \pm 74$ GM at 1445 nm) but remains lower than those reported for other dipolar compounds featuring a longer π-conjugated backbone ($\sigma_{2PA}^{max} = 1500$ GM at 1440 nm)[5b] or for the related squaraine ($\sigma_{2PA}^{max} = 2100$ GM at 1300 nm).[6]

(25) Sheik-Bahae, M.; Said, A. A.; Wei, T.-H.; Hagan, D. J.; Van Stryland, E. W. *IEEE J. Quant. Electron.* **1990**, *26*, 760−769.

(26) Sutherland, R. L. Handbook of Nonlinear Optics, 2nd ed.; Marcel Dekker: New York, 2003; p 583.

(27) The further details of the analysis procedure are previously provided in Tykwinski, R. R.; Kamada, K.; Bykowski, D.; Hegmann, F. A.; Hinkle, R. J. *J. Opt. A, Pure Appl. Opt.* **2002**, *4*, S202−S206 and the supporting information of Ogawa, K.; Ohashi, A.; Kobuke, Y.; Kamada, K.; Ohta, K. *J. Am. Chem. Soc.* **2003**, *125*, 13356−13357.

(28) Mahr, H. Two-Photon Absorption Spectroscopy. In *Quantum Electronics: A Treatise*; Rabin, H., Tang, C. L.; Eds.; Academic Press: New York, 1975; Vol. 1, Nonlinear Optics Part A, Chapter 4, pp 306−308.

(29) Fu, J.; Przhonska, O. V.; Padilha, L. A., Hagan, D. J.; Van Stryland, E. W.; Belfield, K. D.; Bondar, M. V.; Slominsky, Y. L.; Kachkovski, Chem. Phys. **2006**, *321*, 257−268.
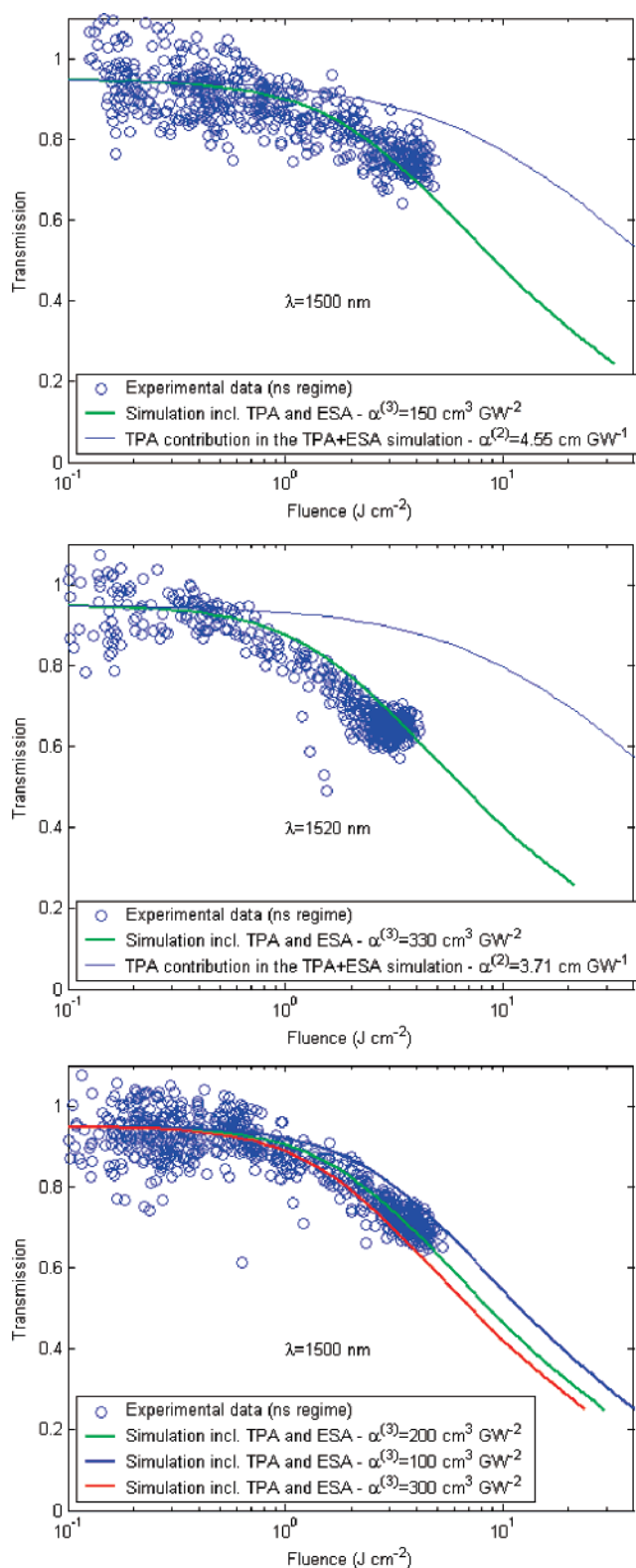
Table 2. 2PA and 3PA Data Using Different Models

			fs Z-scan		
	C^a (g L^{-1})	λ^b (nm)	$\delta_{2PA}{}^c$ (GM)	α_2^{calcd} (cm GW^{-1})	2PA+ ESA $\alpha_3{}^d$ (cm^3 GW^{-2})
2	112.6	1500	530	4.55	150
4	96.5	1500	280	1.59	200
6	92.3	1440	792	5.02	190
		1520	560	3.71	330

[a] Experimental concentration used in optical-limiting measurements. [b] Maximal two-photon absorption wavelength. [c] From femtosecond Z-scan measurement. [d] Determined from OL experiments using complete model.

Optical-Limiting Performance and Mechanism. The high solubility of these compounds allows performing optical-limiting experiments in the NIR spectral range. Nonlinear transmittance measurements were carried out in the 1200−1600 nm range using a tripled Q-switched Nd: YAG laser pumping an optical parametric oscillator (7 ns pulse, 10 Hz) focused in a 2 mm Quartz cell. Typical beam waist $\omega_0 \approx 60\ \mu$m is chosen in order to get high incident energy densities in the sample while achieving a Rayleigh range higher than the 2 mm thickness of the cells and minimizing the influence of thermal defocusing effects (see Experimental Section). The sample is a microfiltrated dichloromethane solution of **1−6** at high concentration (100−350 g L^{-1}). For all samples, variations of the nonlinear transmittance vs the incident laser energy at a given wavelength present the characteristic behavior of an optical limiter: a good transmission at low energy ($T > 0.9$) that significantly decreases at higher energy. A representative example is described in Figure 5, in the case of a concentrated solution of **1** using 1500 nm as fundamental incident wavelength. This is, to the best of our knowledge, the first OL curve at telecommunications wavelength reported in literature for organic molecules; similar curves were obtained for each molecule **1−6**. Experimental points were limited because of the weak power of the incident laser, but an attenuation of 40% of the incident laser beam (incident energy 3×10^{-4} J) can be reached (Figure 5). The relevant role of the concentration on nonlinear transmission properties was studied in the case of **1** at 1500 nm. Upon the sample concentration being decreased from 0.33 to 0.23 mol L^{-1}, a significant flattening of the nonlinear transmission is observed (Figure 5). It must be noted that experimental concentrations used for the OL experiment (Table 2) were not maximal and that more efficient transmission attenuation could be readily reached.

As the theoretical treatments for the open-aperture Z-scan and the nonlinear transmittance measurements are the same as mentioned above, the obtained OL curve was first analyzed with eq. 2 assuming that only the 2PA process is involved in the observation. The simulation curves considering only 2PA process (blue curves of Figure 6), with the two-photon absorption coefficient α_2^{calcd} calculated according to eq. 3 using the σ_{2PA} value determined from the fs Z-scan experiments and with the concentrations of the OL

(30) (a) Swiatkiewicz, J.; Prasad, P. N.; Reinhardt *Opt. Commun.* **1998**, *157*, 135−138. (b) Kim, O.-K.; Lee, K.-S.; Woo, H. Y.; Kim, K.-S; He, G. S.; Swiatkiewicz, J.; Prasad, P. N. *Chem. Mater.* **2000**, *12*, 284−286. (c) Lei, H.; Wang, H. Z.; Wei, Z. C.; Tang, X. J.; Wu, L. Z.; Tung, C. H.; Zhou, G. Y. *Chem. Phys. Lett.* **2001**, *333*, 387−390.


Figure 6. Nonlinear transmittance of **2** (top) and **6** (middle) in concentrated dichloromethane solution (experimental data points and theoretical simulations using simplified 2PA model (red) or complete model including 2PA and ESA (green), including only the 2PA contribution within this latter hypothesis (blue)). Nonlinear transmittance of **4** (bottom) with theoretical simulations using different α_3 coefficients.

samples, exhibit a large deviation from the observed data. Such a large difference was already observed in the nanosecond regime.[30] When the pulse duration is comparable or longer than the lifetime of the excited state of the
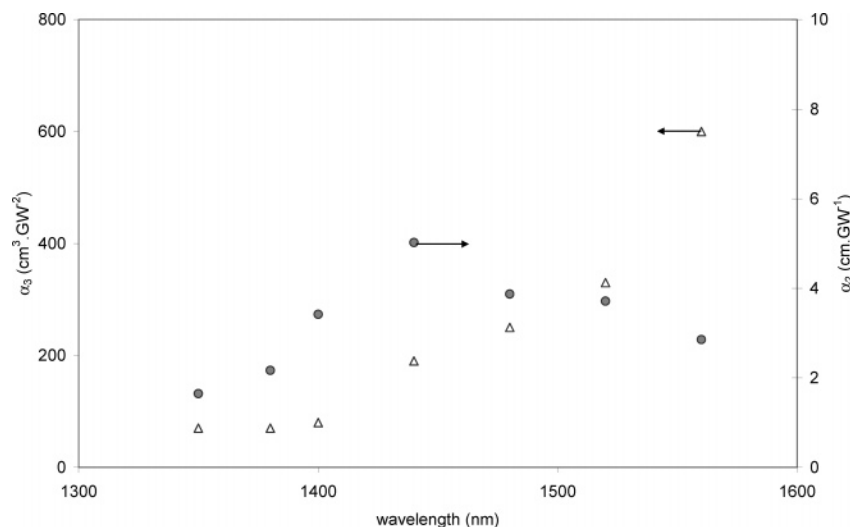
Figure 7. Spectral variation of α_3 coefficient (gray circle) deduced from OL experiment and α_2^{calcd} coefficient calculated from fs Z-scan measurement (open triangle) in the case of **6**.

molecule, higher-order phenomena like 2PA-induced ESA become nonnegligible. The higher-order effect must be taken into account as eq. 4

$$\frac{dI}{dz} = -\alpha_1 I - \alpha_2 I^2 - \alpha_3 I^3 \qquad (4)$$

where α_3 is the three-photon absorption (3PA) coefficient. Any nonlinear absorption process with the same order as 3PA is included in α_3, and thus the 2PA-induced ESA process is included in it. The OL curves were fitted using the extended eq. 4. The α_3 coefficient is determined by numerical resolution of eq. 4 always assuming a Gaussian temporal and spatial incident intensity distribution, as depicted in relationship 5, because eq 4 does not give a simple analytical formulation for T_{nl} such as in eq. 2 when both α_2 and α_3 are nonzero

$$I(z = 0, r, t) = \frac{E}{\pi^{3/2}\tau\omega_0^2} e^{-t^2/\tau^2} e^{-2r^2/\omega_0^2} \qquad (5)$$

where E is the total energy, τ is the HW1/eM pulse duration, and ω_0 is the HW1/e²M beam size.

It is worth noting that similar α_3 determination have already been performed in the visible part of the spectra[31] but, to the best of our knowledge, never in the NIR. Simulations of experimental data using the α_3 approach are represented in green in Figure 6 and are in agreement with experimental curves.

The α_2^{calcd} and α_3 values are reported in the Table 2; for **2**–**6**, 2PA coefficients α_2^{calcd} at the telecommunications wavelength of 1500 nm are between 2 and 5.10^{-11} m W^{-1}, two times lower than those measured for the reference inorganic material GaAs[4] at 1300 nm. The 3PA coefficients at 1500 nm are comprised between 150 and 330 cm³ GW^{-2} for **2**–**6**. The precision in the α_3 determination from eq. 5 is

illustrated, in the case of the polymethine dye **4**, by the bottom part of the Figure 6 in which three fits are represented using α_3 = 100, 200, or 300 cm³ GW^{-2}. Clearly blue and red curves (α_3 = 100 and 300 cm³ GW^{-2}, respectively) represent upper and lower acceptable limits for the experimental data fitting, and therefore the α_3 value could be estimated to 200 ± 100 cm³ GW^{-2}. The spectral distributions of the 3PA and of 2PA coefficients α_3 and α_2^{calcd}, respectively, are compared in Figure 7 between 1300 and 1600 nm for the dipolar compound **6**. Whereas α_2^{calcd} presents a maximum at 1440 nm, α_3 regularly increases up to 1560 nm and the maximum was not reached in this wavelength range. Assuming that the 3PA results from 2PA followed by ESA, this shift in spectral distributions of α_3 and α_2^{calcd} allows to deduce at least two observations: (i) it clearly indicates that the existence of a significant ESA process between 1400 and 1600 nm, which is in agreement with ESA spectra of related polymethine molecules recorded by a pump–probe technique and that present a transition (attributed to $S_1 \rightarrow S_2$) in the NIR;[32] (ii) the best spectral overlap between 2PA and ESA processes, required for optimization of the effective 3PA process, is not reached and could yet be improved in this family of molecules in order to optimize their OL properties.

Conclusion

In conclusion, six cyanine-like chromophores designed for nonlinear absorption in the near IR spectral range have been prepared. These molecules present significant 2PA efficiencies determined by femtosecond Z-scan method, and these systems exhibit optical-limiting properties at telecommunications wavelengths (1500 nm) in nanosecond regime. In the nanosecond pulse regime, the OL experiments were rationalized on the basis of 2PA and the effective 3PA (2PA-induced ESA) processes. Furthermore, this new class of compounds presents many relevant advantages for practical applications

(31) (a) Morel, Y.; Irimia, A.; Najechalski, P.; Kervella, Y.; Stephan, O.; Baldeck, P. L.; Andraud, C. *J. Chem. Phys.* **2001**, *114*, 5391−5396. (b) Anémian, R.; Morel, Y.; Baldeck, P. L.; Paci, B. Kretsch, K. Nunzi, J.-M.; Andraud, C. *J. Mater. Chem.* **2003**, *13*, 2157−2163. (c) Girardot, C.; Lemercier, G.; Andraud, C.; Amari, N.; Baldeck, P. L. *Mol. Cryst. Liq. Cryst.* **2005**, *426*, 197−204.

(32) Negres, R. A.; Przhonska, O. V.; Hagan, D. J.; Van Stryland, E. W.; Bondar, M. V.; Slominsky, Y. L.; Kachkowski, A. D. *IEEE J. Sel. Top. Quantum Electron.* **2001**, *7*, 849−863.

(i) an easy two-step synthesis in a gram scale; (ii) a high solubility in organic solvents due to bulky substituents preventing aggregation, and (iii) a good thermal stability. The existence of several sites allowing functionalization for further use in a biological medium or for a grafting in sol−gel/polymeric matrices will allow the investigation of many different 2PA-based applications in the NIR range, e.g., solid-state optical limiting, biological imaging, signal processing.

Experimental Section

Crystal Structure Analysis for 6. $C_{41}H_{41}N_4ClO$, $M_r = 641.23$, monoclinic, $P2_1/a$, $a = 11.6162(5)$ Å, $b = 17.0136(8)$ Å, $c = 18.6513(9)$ Å, $\beta = 92.615(4)°$, $V = 3682.3(3)$ Å^3, $Z = 4$, $D_x = 1.157$ mg m^{-3}, λ(Mo Kα) = 0.71073 Å, $\mu = 1.40$ cm^{-1}, $F(000) = 1360$, $T = 295(2)$ K. The sample $(0.30 \times 0.28 \times 0.22$ mm$^3)$ was studied on an Oxford Diffraction Xcalibur Saphir 3 diffractometer with graphite-monochromatized Mo Kα radiation. The data collection $(2\theta_{max} = 54°$, omega scan frames via 0.7° omega rotation and 20 s per frame; range HKL, H −15,13, K −18,22, L −23,24) gives 26 700 reflections. The data lead to 8675 independent reflections, of which there are 3336 with $I > 2.0\sigma(I)$. The structure was solved with SIR-97,[33] which revealed the non-hydrogen atoms of the molecule. After anisotropic refinement, all the hydrogen atoms were found with a Fourier difference. The whole structure was refined with SHELXL97[34] by the full-matrix least-square techniques (use of F square magnitude; x, y, z, β_{ij} for O, Cl, C, and N atoms, x, y, z in riding mode for H atoms); 425 variables and 3336 observations with $I > 2.0\sigma(I)$; calcd $w = 1/[\sigma^2(F_o^2) + (0.109P)^2]$ where $P = (F_o^2 + 2F_c^2)/3$ with the resulting $R = 0.057$, $R_w = 0.162$, and $S_w = 0.812$, $\Delta\rho < 0.69$ e Å^{-3}. ORTEP view was made with PLATON 98.[35] All the calculations were performed on a Silicon Graphics Indy computer. Crystallographic data for the structural analysis have been deposited with the Cambridge Crystallographic Data Centre, (CCDC-620269).

Optical-Limiting Setup. The nonlinear transmittance measurements (transmission versus incident energy) were performed with a wavelength tuneable laser source: a tripled Q-switched Nd:YAG laser pumping an optical parametric oscillator delivering 7 ns long pulses. The laser beam was spatially filtered then focused onto the dye solution. Reference energy was taken using a coated wedged flat. The transmitted energy was focused on the signal detector. Typical beam waist $\omega_0 \approx 60$ μm (HW1/e^{2}M) was measured at each test wavelength by imaging the focal plane on a InGaAs camera. The dye sample was adjusted at each wavelength so that its transmission under high flux is minimum (open aperture Z-scan). The incident energy was then controlled by combination of an achromatic half-wave plate and a polarizer. Incident energy was measured using a calibrated Germanium probe (Laser Precision RJP-495) and transmitted energy was measured using pyro-electric probe (Laser Precision RJP-735).

Typical beam waist $\omega_0 \approx 60$ μm was chosen in order to get high incident energy densities in the sample while achieving a Rayleigh range higher than the 2 mm thickness of the cells. The beam characteristics and the experimental setup were chosen to minimize the influence of defocusing effects:

• The pulse repetition rate (10 Hz) is much smaller than the reciprocal thermal diffusion time in the cell ($\tau_d = \omega_0^2/D \approx 4$ μs).

• The solvent (dichloromethane) and the beam waist are chosen in order to get a long acoustic transient time ($\tau_{ac} = \omega_0/C_s = 60$ ns, where C_s is the speed of sound) : the pulse width is small compared to the acoustic transient time. Therefore, the sensitivity of the measurement to nonlinear refraction is reduced.[36]

• The collecting lens aperture (which is twice the size of the beam in linear regime) and the detector size were chosen so that all the transmitted light is collected and focused onto the detector even under high incident flux.

With these experimental precautions, no aperture losses due to defocusing effects were observed.

General Procedures. All reactions were routinely performed under argon. NMR spectra (^{1}H, ^{13}C) were recorded at room temperature on a BRUKER AC 200 operating at 200.13 MHz and 50.32 for ^{1}H and ^{13}C, respectively, and on a VARIAN Unity Plus operating at 499.84 MHz for ^{1}H NMR. Data are listed in parts per million (ppm) and are reported relative to tetramethylsilane (^{1}H, ^{13}C), residual solvent peaks being used as internal standard (CHCl$_3$ ^{1}H, 7.26 ppm; ^{13}C, 77.36 ppm). UV−visible spectra were recorded on a Jasco V-550 spectrophotometer in diluted dichloromethane solution (ca. 10^{-5} mol L^{-1}). Infra-Red spectra were recorded on a Mattson 3000 spectrometer using KBR Pellets. Thermogravimetric analysis (TGA) measurements were recorded on a NIETZSCH STA 409 PC/PG under a nitrogen atmosphere. High-resolution mass spectrometry measurements were performed at the Service Central d'Analayse du CNRS (Vernaison, France) and at the Centre Commun de Spectrométrie de Masse (UCBL, Villeurbanne, France) and elemental analysis by the Service Central d'Analyze du CNRS (Vernaison, France). Column Chromatography was performed on Merck Gerduran 60 (40−63 μm) silica using dichloromethane as eluent. Bis-aldehyde **A**[11] and tricyanofurane[37] were prepared according to published procedures.

Dye 1. 1-hexyl-2-methyl-benzothiazolium bromide (2.5 g, 8 mmol, 3.6 equiv.) and **A** (500 mg) were dissolved in absolute ethanol:pyridine (4:1, 25 mL) under argon. The solution was refluxed for 20 h. After evaporation of the solvent, the mixture was dissolved in dichloromethane (30 mL) washed with water, dried with Na$_2$SO$_4$, and filtered, and the solvent was evaporated. The crude was washed thoroughly with diethyl ether and pentane to afford a green solid (1.2 g, 60%). ^{1}H NMR (200.13 MHz, CDCl$_3$): δ 0.6−1.0 (9H, m), 1.13 (9H, s), 1.2−1.7 (13H, m), 1.7−2.0 (12H, m), 2.02 (3H, s), 2.28 (1H, dd. $^2J = 13$ Hz. $^3J = 13$ Hz), 2.36 (1H, dd. $^2J = 13$ Hz. $^3J = 13$ Hz), 2.9−3.0 (1H+1H, m), 4.2−4.6 (6H, m), 6.38 (1H, d, $^3J = 14$ Hz), 6.42 (1H, d, $^3J = 14$ Hz), 6.9−7.6 (12H, m), 8.10 (1H, d, $^3J = 14$ Hz), 8.13 (1H, d, $^3J = 14$ Hz). HRMS (ESI+) M = 874.4838 (calcd for $C_{54}H_{72}N_3OS_3$, 874.4836). Anal. Calcd for $C_{54}H_{72}N_3BrOS_3\cdot H_2O$: C, 66.70; H, 7.62; N, 4.32. Found: C, 66.26; H, 7.36; N, 4.16. UV−vis (CH$_2$Cl$_2$): $\lambda_{max} = 825$ nm ($\epsilon_{max} = 240\ 000$ L mol^{-1} cm^{-1}).

Dye 2. 1-benzyl-2-methyl-benzothiazolium bromide (2.55 g, 8 mmol, 3.6 equiv) and **A** (500 mg) were dissolved in absolute ethanol:pyridine (4:1, 25 mL) under argon. The solution was refluxed for 20 h. After evaporation of the solvent, the mixture was dissolved in dichloromethane (30 mL), washed with water, dried with Na$_2$SO$_4$, and filtered, and the solvent was evaporated. The crude was washed thoroughly with ethyl acetate and pentane to afford a green solid (1.5 g, 70%). ^{1}H NMR (499.84 MHz, CD$_2$-Cl$_2$): δ 1.03 (9H, s), 1.52 (1H, m), 2.06 (3H, s), 2.16 (1H, dd, $^2J = 13$ Hz, $^3J = 12$ Hz), 2.18 (1H, dd, $^2J = 13$ Hz, $^3J = 12$ Hz),

(33) Altomare, A.; Burla, M. C.; Camalli, M.; Carscarano, G.; Giacovazzo, C.; Guagliardi, A.; Moliterni, A. G. G.; Polidori, G.; Spagna, R. *J. Appl. Crystallogr.* **1998**, *31*, 74−77.
(34) Sheldrick, G. M. *SHELX93, Program for the Refinement of Crystal Structures*; University of Göttingen: Göttingen, Germany, 1993.
(35) Spek, A. L. *PLATON, A Multipurpose Crystallographic Tool*; Utrecht University: Utrecht, The Netherlands, 1998.
(36) Kovsh, D. I.; Yang, S.; Hagan, D. J.; Van Stryland, E. W. *Appl. Opt.* **1999**, *38*, 5168−5180.
(37) Gopolan, P.; Katz, H. E.; McGee, D. J.; Erben, C.; Zielinsky, T.; Bousquet, D.; Muller, D.; Grazul, J.; Olsson, Y. *J. Am. Chem. Soc.* **2004**, *126*, 1741−1747.

Near-IR Nonlinear Absorbing Chromophores

Chem. Mater., Vol. 19, No. 22, 2007 5335

2.71 (1H, dd, ^2J=13 Hz, ^3J= 1 Hz), 2.74 (1H, dd, ^2J = 13 Hz, ^3J = 1 Hz), 4.2 (1H, d, ^2J = 15 Hz), 5.65 (4H, m), 5.92 (1H, d, ^2J = 15 Hz), 6.41 (1H, d, ^3J = 14 Hz), 6.42 (1H, d, ^3J = 14 Hz), 6.70 (1H, d, ^3J = 7,5 Hz), 6.92 (1H, d, ^3J = 7 Hz), 6.99 (1H, m), 7.05−7.65 (24 H, m), 8.17 (1H, d, ^3J = 14 Hz), 8.19 (1H, d, ^3J = 14 Hz). HRSM (ESI+) : M$^+$ = 892.3429 (calcd for $C_{57}H_{54}N_3OS_3$, 892.3423). Anal. Calcd for $C_{57}H_{54}N_3BrOS_3 \cdot H_2O$: C, 69.13; H, 5.66; N, 4.24. Found: C, 68.99; H 5.45; N, 4.02. UV−vis (CH_2Cl_2) λ_{max} = 833 nm (ϵ_{max} = 275 000 L mol^{-1} cm^{-1}).

Dye 3. 1-hexyl-2,3,3-trimethylindolenium iodide (1.070 g, 2.8 mmol, 2.1 equiv.) and **A** (0.300 g, 1.3 mmol, 1 equiv.) were dissolved in absolute ethanol (30 mL) under argon. After addition of pyridine (0.26 mL, 3.2 mmol, 2.5 equiv) the mixture was heated at 40 °C for 15 h. The resulting green solution was cooled to room temperature ,and dichloromethane (50 mL) was added. The organic layer was washed with an aqueous solution of dilute HCl, water and brine, dried with Na$_2$SO$_4$ filterd and the solvent was evaporated under vacuum. The crude was dissolved in the minimum amount of dichloromethane and precipitated by addition of pentane. The desired product was obtained by filtration, as a green solid (0.740 g, 70%). ^{1}H NMR (200.13 MHz, CDCl$_3$): δ 0.93 (6H, m), 1.11 (9H, s), 1.4 (13H, m), 1.75 (12H, s), 1.80−1.96 (4H, m), 2.25 (2H, dd, ^3J = 12 Hz, ^2J = 12 Hz), 2.90 (2H, d, ^3J = 12 Hz), 4.10 (4H, t, ^3J = 7 Hz), 6.15 (2H, d, ^3J = 14 Hz), 7.21 (2H, dd, ^3J = 8 Hz), 7.32 (2H, d, ^3J = 8 Hz), 7.40−7.50 (4H, m), 8.43 (2H, d, ^3J = 14 Hz). ^{13}C NMR (50.32 MHz, CD$_2$Cl$_2$): δ 13.7, 22.4, 26.6, 27.1, 27.4, 27.8, 27.9, 31.3, 32.3, 42.3, 44.7, 49.4, 100.7, 110.9, 122.3, 125.4, 127.1, 128.7, 141.1, 142.1, 144.4, 150.5, 172.6. HRMS (ESI+): M$^+$ = 679.4781 (calcd for $C_{46}H_{64}N_2Cl$, 679.4758). Anal. Calcd for: $C_{46}H_{64}N_2ClI$: C, 68.43; H, 7.99; N, 3.47. Found: C, 68.59; H, 8.08; N, 3.25. UV−vis (CH_2Cl_2): λ_{max} = 791 nm (ϵ_{max} = 355 000 L mol^{-1} cm^{-1}).

Dye 4. 1-benzyl-2,3,3-trimethylindolenium bromide (2.700 g, 8.2 mmol, 2.1 equiv) and **A** (0.891 g, 3.9 mmol, 1 equiv) were dissolved in absolute ethanol (50 mL) under argon. After addition of pyridine (0.8 mL, 9.9 mmol, 2.5 equiv), the mixture was heated at 40 °C for 15 h. The resulting green solution was cooled to room temperature and dichloromethane (100 mL) was added. The organic layer was washed with an aqueous solution of dilute HCl, water, brine, dried with Na$_2$SO$_4$, and filtered, and the solvent was evaporated under vacuum. The crude was dissolved in the minimum amount of dichloromethane and precipitated by addition of pentane. The desired product was obtained by filtration, as a green solid (2.200 g, 72%). ^{1}H NMR (200.13 MHz, CDCl$_3$): δ 0.98 (9H, s), 1.4 (1H, m), 1.74 (12H, s), 2.05 (2H, dd, ^3J = 13 Hz, ^2J = 13 Hz), 2.6 (2H, dd, ^3J = 2 Hz, ^2J = 13 Hz), 5.43 (2H, d, ^2J = 16 Hz), 5.52 (2H, d, ^2J = 16 Hz), 6.18 (2H, d, ^3J = 14 Hz), 7.2−7.5 (18H, m), 8.23 (2H, d, ^3J = 14 Hz).^{13}C NMR (50.32 MHz, CDCl$_3$): δ 27.3, 28.1, 28.2, 32.3, 41.9, 48.4, 49.3, 102.2, 111.1, 122.4, 125.5, 126.6, 128.2, 128.3, 129.0, 129.2, 134.2, 140.8, 142.7, 144.2, 150.6, 172.5. HRMS (ESI+): M$^+$ = 691.3842 (calcd for $C_{48}H_{52}N_2Cl$, 691.3814). Anal. Calcd for $C_{48}H_{52}N_2BrCl$: C, 74.65; H, 6.79; N, 3.63,. Found: C, 74.08; H, 6.90; N, 3.33. UV−vis (CH_2Cl_2): λ_{max} = 794 nm (ϵ_{max} = 350 000 L mol^{-1} cm^{-1}).

Dye 5. A (180 mg, 0.78 mmol, 1 equiv) and tricyanofurane (155 mg, 1 equiv) were dissolved in *n*-butanol (15 mL) under argon. After addition of pyridine (0.06 mL, 0.78 mmol, 1 equiv), the

mixture was heated at 100 °C for 1.5 h. A solution of 1-hexyl-2,3,3-trimethylindolenium iodide (376 mg, 1.2 equiv.) in *n*-butanol (10 mL) was added. The solution was then heated for 3 h at 100 °C. The resulting green solution was cooled to room temperature and dichloromethane (50 mL) was added. The organic layer was washed with an aqueous solution of dilute HCl, water, brine, dried with Na$_2$SO$_4$, and filtered. and the solvent was evaporated under a vacuum. Purification by column chromatography on silica gel (eluent, dichloromethane) afforded a green solid (170 mg, 35%). ^{1}H NMR (200.13 MHz, CDCl$_3$): δ 0.9 (m, 3H), 1.04 (s, 9H), 1.2−1.6 (m, 9H), 1.67 (s, 6H), 1.75 (s, 6H), 2.07 (m, 1H+1H), 2.81 (dd, 1H+1H), 3.82 (t, 2H, ^3J = 7 Hz), 5.70 (d, 1H, ^3J = 13 Hz), 6.33 (d, 1H, ^3J = 15 Hz), 6.85 (d, 1H, ^3J = 8 Hz), 7.04 (dd, 1H, ^3J = 8 Hz), 7.25−7.32 (m, 2H), 7,95 (d, 1H, ^3J = 13 Hz), 8.12 (d, 1H, ^3J = 15 Hz). ^{13}C NMR (50.32 MHz, CDCl$_3$): δ 14.4, 22.9, 27.0, 27.2, 27.5, 27.7, 27.8, 28.0, 28.6, 28.8, 31.8, 32.8, 42.8; 43.8, 48.1, 93.4, 96.2, 96.7, 108.7, 110.8, 112.3, 112.9, 113.7, 122.5, 123.1, 126.4, 128.1, 128.7, 137.2, 140.3, 143.7, 144.7, 147.7, 166.2, 173.4, 176.8. HRMS (ES+) MH$^+$ = 635.3546 (calcd for $C_{40}H_{47}N_4$-OCl, 635.3517). UV−vis (CH_2Cl_2): λ_{max} = 831 nm (ϵ_{max} = 112 000 L mol^{-1} cm^{-1}).

Dye 6. A (172 mg, 0.75 mmol, 1 equiv) and tricyanofurane (151 mg, 1 equiv) were dissolved in *n*-butanol (15 mL) under argon. After addition of pyridine (0.06 mL, 0.78 mmol, 1.1 equiv), the mixture was heated at 100 °C for 1.5 h. A solution of 1-benzyl-2,3,3-trimethylindolenium bromide (300 mg, 1.2 equiv.) in *n*-butanol (10 mL) was added. The solution was then heated for 3 h at 100 °C. The resulting green solution was cooled to room temperature and dichloromethane (50 mL) was added. The organic layer was washed with an aqueous solution of dilute HCl, water, brine, dried with Na$_2$SO$_4$, and filtrated. The solvent was evaporated under a vacuum. Purification by column chromatography on silica gel (eluent, dichloromethane) afforded a green solid (300 mg, 30%). ^{1}H NMR (200.13 MHz, CDCl$_3$): δ 0.97 (s, 9H), 1.49 (m, 1H), 1.70 (s, 6H), 1.75 (s, 6H), 2.08 (m, 1H+1H), 2.65 (m, 1H+1H), 4.93 (d, 1H, ^2J = 16 Hz), 4.99 (d, 1H, ^2J = 16 Hz), 5.63 (d, 1H, ^3J = 13 Hz), 6.35 (d, 1H, ^3J = 16 Hz), 6.88 (d, 1H, ^3J = 8 Hz), 7.06 (d, 1H, ^3J = 8 Hz), 7.1−7.4 (m, 7H), 7.85 (d, 1H, ^3J = 13 Hz), 8.08 (d, 1H, ^3J = 16 Hz). ^{13}C NMR (50.32 MHz, CDCl$_3$): δ 27.1, 27.2, 27.4, 27.6, 28.4, 28.5, 32.3, 42.3, 47.0, 47.4, 94.0, 96.5, 96.9, 108.1, 111.1, 111.6, 112.3, 113.1, 122.2, 122.6, 126.5, 126.7, 128.0, 128.1, 128.4, 129.2, 135.3, 135.7, 139.6, 143.9, 144.4, 146.9, 164.8, 173.2, 176.2. MS (ESI+): MH$^+$ = 641.3047 (calcd for $C_{41}H_{41}ClN_4O$, 641.3042). Anal. Calcd for $C_{41}H_{41}ClN_4O$: C, 76.79; H, 6.44; N, 8.74. Found: C, 76.61; H, 6.53; N, 8.45. UV−vis (CH_2Cl_2): λ_{max} = 810 nm (ϵ_{max} = 91 000 L mol^{-1} cm^{-1}). IR (KBr pellet) $\nu_{C\equiv N}$ 2218 cm^{-1}.

Supporting Information Available: Crystallographic data of compound **6** in CIF format. This material is available free of charge via the Internet at http://pubs.acs.org.